Surface Parameterization using Riemann Surface Structure

Yalin Wang
Mathematics Department
UCLA
ylwang@math.ucla.edu

Xianfeng Gu
Comp. Sci. Department
SUNY at Stony Brook
gu@cs.sunysb.edu

Kiralee M. Hayashi
Lab. of Neuro Imaging
UCLA School of Medicine
khayashi@loni.ucla.edu

Tony F. Chan
Mathematics Department
UCLA
chan@math.ucla.edu

Paul M. Thompson
Laboratory of Neuro Imaging
UCLA School of Medicine
thompson@loni.ucla.edu

Shing-Tung Yau
Mathematics Department
Harvard University
yau@math.harvard.edu

Abstract

We propose a general method that parameterizes general surfaces with complex (possible branching) topology using Riemann surface structure. Rather than evolve the surface geometry to a plane or sphere, we instead use the fact that all orientable surfaces are Riemann surfaces and admit conformal structures, which induce special curvilinear coordinate systems on the surfaces. We can then automatically partition the surface using a critical graph that connects zero points in the global conformal structure on the surface. The trajectories of iso-parametric curves canonically partition a surface into patches. Each of these patches is either a topological disk or a cylinder and can be conformally mapped to a parallelogram by integrating a holomorphic 1-form defined on the surface. The resulting surface subdivision and the parameterizations of the components are intrinsic and stable. For surfaces with similar topology and geometry, we show that the parameterization results are consistent and the subdivided surfaces can be matched to each other using constrained harmonic maps. The surface similarity can be measured by direct computation of distance between each pair of corresponding points on two surfaces. To illustrate the technique, we computed conformal structures for anatomical surfaces in MRI scans of the brain and human face surfaces. We found that the resulting parameterizations were consistent across subjects, even for branching structures such as the ventricles, which are otherwise difficult to parameterize. Our method provides a surface-based framework for statistical comparison of surfaces and for generating grids on surfaces for PDE-based signal processing.

1. Introduction

Surface-based modeling is valuable for shape analysis, surface matching and object recognition. For medical imaging applications, it is useful to help analyze anatomical shape, to statistically combine or compare 3D anatomical models across subjects, and to map functional imaging parameters onto anatomical surfaces. Parameterization of these surface models involves computing a smooth (differentiable) one-to-one mapping of regular 2D coordinate grids onto the 3D surfaces, so that numerical quantities can be computed easily from the resulting models. Even so, it is often difficult to smoothly deform a complex 3D surface to a sphere or 2D plane without substantial angular or area distortion. Here we present a new method to parameterize general surfaces based on their Riemann surface structure. By contrast with variational approaches based on surface inflation, our method can parameterize surfaces with arbitrary complexity including branching surfaces not topologically homeomorphic to a sphere (higher-genus objects) while formally guaranteeing minimal distortion.

1.1. Previous Work

Thirion [14] uses the extremal mesh to describe 3D smooth surfaces. The extremal mesh is the graph of a surface whose vertices are the extremal points and whose edges are the extremal lines. It is invariant with respect to rigid transformations. Davies et al. [1] describe a method for building statistical shape models by posing a correspondence problem to identify a consistent parameterization for each shape in a training set. Several recent advances in surface parameterization have been based on solving a discrete Laplace system [11, 3]. Lévy et al. [10] describe a technique for finding conformal mappings by least squares minimiza-

tion of the *conformal energy*, and Desbrun et al. [2] formulate a theoretically equivalent method for discrete conformal parameterization. Sheffer et al. [13] give an angle-based flattening method for conformal parameterization. Gu and Yau [6] consider construction of a global conformal structure for a manifold of arbitrary topology by finding a basis for holomorphic differential forms, based on Hodge theory.

Brain surface parameterization has been studied intensively. Schwartz et al. [12] compute quasi-isometric flat maps of the cerebral cortex. Hurdal and Stephenson [8] report a discrete mapping approach that uses circle packings to produce "flattened" images of cortical surfaces. Haker et al. [7] implement a finite element approximation for parameterizing brain surfaces via conformal mappings. Gu et al. [4] propose a method to find a unique conformal mapping between any two genus zero manifolds by minimizing the harmonic energy of the map. They demonstrate this method by conformally mapping the cortical surface to a sphere.

1.2 Theoretical Background and Definitions

A *manifold* of dimension n is a connected Hausdorff space M for which every point has a neighborhood U that is homeomorphic to an open subset V of R^n. Such a homeomorphism $\phi : U \to V$ is called a coordinate chart. An *atlas* is a family of charts $\{U_\alpha, \phi_\alpha\}$ for which U_α constitute an open covering of M (Figure 1). Suppose $\{U_\alpha, \phi_\alpha\}$ and

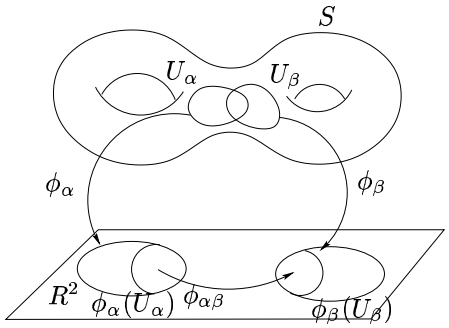

Figure 1. The Structure of a Manifold. An atlas is a family of charts that jointly form an open covering of the manifold.

$\{U_\beta, \phi_\beta\}$ are two charts on a manifold S, $U_\alpha \cap U_\beta \neq \Phi$, then the chart transition is defined as $\phi_{\alpha\beta} : \phi_\alpha(U_\alpha \cap U_\beta) \to \phi_\beta(U_\alpha \cap U_\beta)$. An atlas $\{U_\alpha, \phi_\alpha\}$ on a manifold is called *differentiable* if all chart transitions are differentiable of class C^∞. A chart is called *compatible* with a differentiable atlas if adding this chart to the atlas still yields a differentiable atlas. The set of all charts compatible with a given differentiable atlas yields a *differentiable structure*. A *differentiable manifold* of dimension n is a manifold of dimension n together with a differentiable structure.

For a manifold M with an atlas $\mathcal{A} = \{U_\alpha, \phi_\alpha\}$, if all chart transition functions, $\phi_{\alpha\beta} = \phi_\beta \circ \phi_\alpha^{-1} : \phi_\alpha(U_\alpha \cap U_\beta) \to \phi_\beta(U_\alpha \cap U_\beta)$, are holomorphic, then $\mathcal{A}$ is a conformal atlas for M. A chart $\{U_\alpha, \phi_\alpha\}$ is *compatible* with an atlas $\mathcal{A}$, if the union $\mathcal{A} \cup \{U_\alpha, \phi_\alpha\}$ is still a conformal atlas.

Two conformal atlases are compatible if their union is still a conformal atlas. Each conformal compatible equivalence class is a conformal structure. A 2-manifold with a conformal structure is called a *Riemann surface*. It has been proven that all metric orientable surfaces are Riemann surfaces.

Holomorphic and meromorphic functions and differential forms can be generalized to Riemann surfaces by using the notion of conformal structure. For example, a *holomorphic* 1-form ω is a complex differential form, such that in each local frame $z_\alpha = (u_\alpha, v_\alpha)$, the parametric representation is $\omega = f(z_\alpha)dz_\alpha$, where $f(z_\alpha)$ is a holomorphic function. On a different chart $\{U_\beta, \phi_\beta\}$, $\omega = f(z_\alpha(z_\beta))\frac{dz_\alpha}{dz_\beta}dz_\beta$. For a genus g closed surface, all holomorphic 1-forms form a real $2g$ dimensional linear space.

At a *zero point* $p \in M$ of a holomorphic 1-form ω, any local parametric representation $\omega = f(z_\alpha)dz_\alpha, f|_p = 0$. According to the Riemann-Roch theorem, in general there are $2g - 2$ zero points for a holomorphic 1-form defined on a surface of genus g.

A holomorphic 1-form induces a special system of curves on a surface, the so-called *conformal net*. A curve $\gamma \subset M$ is called a horizontal trajectory of ω, if $\omega^2(d\gamma) \geq 0$; similarly, γ is a vertical trajectory if $\omega^2(d\gamma) < 0$. The horizontal and vertical trajectories form a web on the surface. The trajectories that connect zero points, or a zero point with the boundary are called *critical trajectories*. The critical horizontal trajectories form a graph, which is called the *critical graph*. In general, the behavior of a trajectory may be very complicated, it may have infinite length and may be dense on the surface. If the critical graph is finite, then all the horizontal trajectories are finite. The critical graph partitions the surface into a set of non-overlapping patches that jointly cover the surface, and each patch is either a topological disk or a topological cylinder. Each patch $\Omega \subset M$ can be mapped to the complex plane using the following formulae. Suppose we pick a base point $p_0 \in \Omega$, and any path γ that connects p_0 to p. Then if we define $\phi(p) = \int_\gamma \omega$, the map ϕ is conformal, and $\phi(\Omega)$ is a parallelogram. We say ϕ is the conformal parameterization of M induced by ω. ϕ maps the vertical and the horizontal trajectories to iso-u and iso-v curves respectively on the parameter plane. The structure of the critical graph and the parameterizations of the patches are determined by the conformal structure of the surface. If two surfaces share similar

topologies and geometries, they can support consistent critical graphs and segmentations (i.e. surface partitions), and the parameterizations are consistent as well. Therefore, by matching their parameter domains, the entire surfaces can be directly matched in 3D. This generalizes prior work in medical imaging that has matched surfaces by computing a smooth bijection to a single canonical surface, such as a sphere or disk.

A Riemannian metric is a differential quadratic form on a differential manifold. On each chart $\{U_\alpha, \phi_\alpha\}$, it can be represented as $ds^2 = E(u,v)du^2 + 2F(u,v)dudv + G(u,v)dv^2$. A special conformal structure can be chosen, such that the local parametric representation of Riemannian metric is $ds^2 = \lambda(u,v)(du^2 + dv^2)$. In this case, the local coordinates of each chart are also called *isothermal coordinates*, and $\lambda(u,v)$ is called the *conformal factor*.

Suppose $\Omega_1, \Omega_2 \subset \mathcal{R}^2$ are two planar domains. A map $\phi : \Omega_1 \to \Omega_2$, known as the *harmonic energy*, measures the stretching of ϕ, and is defined as $E_\phi = \int_{\Omega_1} ||\nabla\phi||^2 dudv$. A *harmonic map* ϕ minimizes the harmonic energy. Intuitively, we can imagine Ω_1 is made of rubber and deformed onto Ω_2. Any map will introduce an elastic stretching energy, but harmonic maps are those that minimize the stretching energy (as defined by the functional) among all possible mappings.

This paper takes the advantage of conformal structures of surfaces, consistently segments them and parameterizes the patches using a holomorphic 1-form. The parametric domains are then matched using harmonic maps.

We call the process of finding critical graph and segmentation as the *holomorphic flow segmentation*, which is completely determined by the geometry of the surface and the choice of the holomorphic 1-form. (Note that this differs from the typical meaning of segmentation in medical imaging, and is concerned with the segmentation, or partitioning, of a general surface). Computing holomorphic 1-forms is equivalent to solving elliptic differential equations on the surfaces, and in general, elliptic differential operators are stable. Therefore the resulting surface segmentations and parameterizations are intrinsic and stable, and are applicable for matching noisy surfaces derived from medical images.

2. Holomorphic Flow Segmentation

To compute the holomorphic flow segmentation of a surface, first we compute the conformal structure of the surface; then we select one holomorphic differential form, and locate the zero points on it. By tracing horizontal trajectories through the zero points, the critical graph can be constructed and the surface is divided into several patches. Each patch can then be conformally mapped to a planar parallelogram by integrating the holomorphic differential form.

In our work, surfaces are represented as triangular meshes, namely piecewise polygonal surfaces. The computations with differential forms are based on solving elliptic partial differential equations on surfaces using the finite element method.

2.1 Computing Conformal Structures

A method for computing the conformal structure of a surface was introduced in [5]. Suppose M is a closed genus $g > 0$ surface with a conformal atlas $\mathcal{A}$. The conformal structure $\mathcal{A}$ induces holomorphic 1-forms; all holomorphic 1-forms form a linear space $\Omega(M)$ of dimension $2g$ which is isomorphic to the first cohomology group of the surface $H^1(M, \mathcal{R})$. The set of holomorphic 1-forms determines the conformal structure. Therefore, computing conformal structure of M is equivalent to finding a basis for $\Omega(M)$.

The holomorphic 1-form basis $\{\omega_i, i = 1, 2, \cdots, 2g\}$ is computed as follows: compute the homology basis, find the dual cohomology basis, diffuse the cohomology basis to a harmonic 1-form basis, and then convert the harmonic 1-form basis to holomorphic 1-form basis by using the Hodge star operator. The details of the computation are given in [5]. In terms of data structure, a holomorphic 1-form is represented as a vector-valued function defined on the edges of the mesh $\omega_i : K_1 \to R^2, i = 1, 2 \cdots, 2g,$.

2.2 Selecting the Optimal Holomorphic 1-form

Given a Riemann surface M, there are infinitely many holomorphic 1-forms, but each of them can be expressed as a linear combination of the basis elements. We define a canonical conformal parameterization as any linear combination of the set of holomorphic basis functions ω_i, $i = 1, ..., g$. They satisfy $\int_{\zeta_i} \omega_j = \delta_i^j$, where $\zeta_i, i = 1, ...n$ are homology bases and δ_i^j is the Kronecker symbol. Then we compute a *canonical conformal parameterization* $\omega = \sum_{i=1}^n \omega_i$.

We select a specific parameterization one that maximizes the uniformity of the induced grid over the entire domain using the algorithms introduced in [9], for the purpose of locating zero points in the next step.

2.3 Locating Zero Points

For surface with genus $g > 1$, any holomorphic 1-form ω has $2g - 2$ zero points. The horizontal trajectories through the zero points will partition the surface into several patches. Each patch is either a topological disk or a cylinder, and can be conformally parameterized by ω using $\phi(p) = \int_\gamma \omega$.

Estimating the Conformal Factor Suppose we already have a global conformal parameterization, induced by a holomorphic 1-form ω. Then we can estimate the conformal factor at each vertex, using the following formulae:

$$\lambda(v) = \frac{1}{n} \sum_{[u,v] \in K_1} \frac{|\omega([u,v])|^2}{|r(u) - r(v)|^2}, u, v \in K_0, \quad (1)$$

where n is the valence of vertex v.

Locating Zero Points We find the cluster of vertices with relatively small conformal factors (the lowest $5-6\%$). These are candidates for zero points. We cluster all the candidates using the metric on the surface. For each cluster, we pick the vertex that is closest to the center of gravity of the cluster, using the surface metric to define geodesic distances.

Because the triangulation is finite and the computation is an approximation, the number of zero points may not equal the Euler number. In this case, we refine the triangulation of the neighborhood of the zero point candidate and refine the holomorphic 1-form ω.

2.4. Holomorphic Flow Segmentation

Tracing Horizontal Trajectories Once the zero points are located, the horizontal trajectories through them can be traced.

First we choose a neighborhood U_v of a vertex v representing a zero point, U_v is a set of neighboring faces of v, then we map it to the parameter plane by integrating ω. Suppose a vertex $w \in U_v$, and a path composed by a sequence of edges on the mesh is γ, then the parameter location of w is $\phi(w) = \int_\gamma \omega$.

The map $\phi(w)$ is a piecewise linear map. Then the horizontal trajectory is mapped to the horizontal line $y = 0$ in the plane. We slice $\phi(U_v)$ using the line $y = 0$ by edge splitting operations. Suppose the boundary of $\phi(U_v)$ intersects $y = 0$ at a point v', then we choose a neighborhood of v' and repeat the process.

Each time we extend the horizontal trajectory and encounter edges intersecting the trajectory, we insert new vertices at the intersection points, until the trajectory reaches another zero point or the boundary of the mesh. We repeat the tracing process until each zero point connects 4 horizontal trajectories.

Critical Graph Given a surface M and a holomorphic 1-form ω on M, we define the graph $G(M, \omega) = \{V, E, F\}$, as the critical graph of ω. Here V is the set of zero points of ω, E is the set of horizontal trajectories connecting zero points or the boundary segments of M, and F is the set of surface patches segmented by E.

Given two surfaces with similar topologies and geometries, by choosing appropriate holomorphic 1-forms, we can obtain isomorphic critical graphs, which will be used for patch-matching described in the next section.

3. Experimental Results

We tested our algorithm on various surfaces, including a synthetic geometric example, human face surfaces and anatomic surfaces extracted from 3D MRI scans of the brain. Figure 2(a)-(d) shows a closed genus 2 surface. We

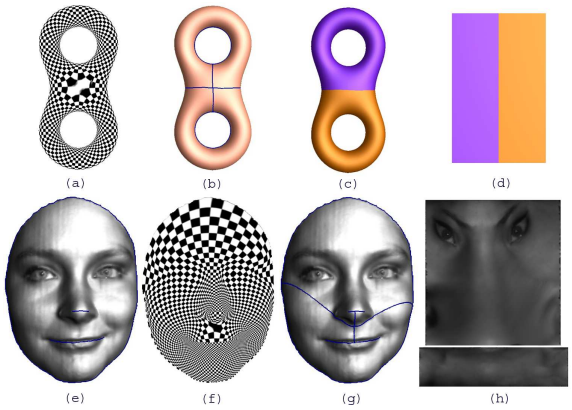

Figure 2. Holomorphic flow segmentation results on a synthetic surface and a surface model of the face. With two cuts introduced (e), the face surface becomes an open boundary genus 2 surface. (a) and (f) are conformal parameterizations of the two surfaces. (b) and (g) show horizontal trajectories. (d) and (h) are the two rectangles to which two segments in (c) and (g) are conformally mapped, respectively.

visualized the conformal structure by projecting a checkerboard image back onto the surface (Figure 2(a)). There is a zero point shown in Figure 2(a). Another zero point is on the back of the "figure-eight" shaped surface and is symmetric to this zero point. The traced horizontal and vertical trajectories are shown in Figure 2(c). From the computed conformal structure, the "figure-eight" surface can be segmented into two patches (Figure 2(c)). Each patch can then be conformally mapped to a rectangle (Figure 2(d)). Figure 2(e)-(g) shows experimental results for a human face surface. The surface was built with a high resolution, real-time 3D face acquisition [15]. For a detailed studies of geometrical differences between faces (e.g. for face tracking and recognition applications), we can optimize the conformal parameterization by modifying the topology of the face model. We introduce two cuts on the tip of the nose and mouth (the blue lines in (e)), so a human face model becomes an open-boundary genus two surface. (f) shows its conformal structure and there is a zero point between the nose and mouth illustrated by the black dot. The horizontal trajectory curves are shown in (g). We can conformally map the face surface to two rectangles (h). Compared with other face surface parameterization methods, our method can represent the surface with minimal distortion.

Shape analysis of the lateral ventricles - a structure in the brain - is of great interest in the study of psychiatric illnesses, including schizophrenia, and in degenerative dis-

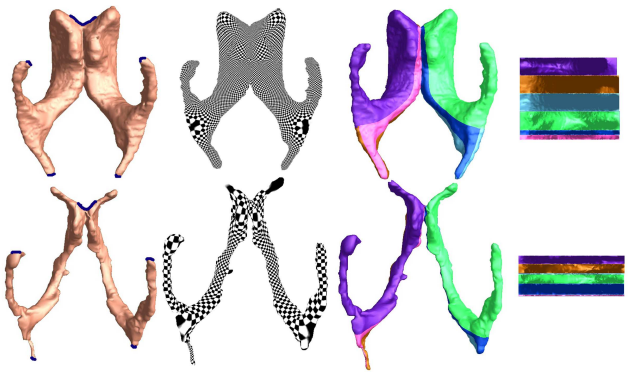

Figure 3. Surface parameterization results for the lateral ventricles. The upper row shows models parameterized using holomorphic 1-forms, for a 65-year-old subject with HIV/AIDS and the lower row shows the same maps computed for a healthy 21-year-old control subject. The left column shows that 5 cuts are introduced and they convert the lateral ventricular surface into a genus 4 surface. The computed conformal structure, holomorphic flow segmentation and their associated parameter domains are also shown.

eases such as Alzheimer's disease. These structures are often enlarged in disease and can provide sensitive measures of disease progression. For the lateral ventricular surface in each brain hemisphere, we introduce five cuts. Since these cutting positions are at the ends of the frontal, occipital, and temporal horns of the ventricles, they can potentially be located automatically. The left column in Figure 3 shows 5 cuts introduced on two subjects ventricular surfaces. After the cutting, the surfaces become open boundary genus 4 surfaces. The rest of Figure 3 shows parameterizations of the lateral ventricles of the brain. The upper row shows the results of parameterizing a ventricular surface for a 65-year-old patient with HIV/AIDS (note the disease-related enlargement) and the lower row shows the results for the ventricular model of a 21-year-old control subject. The surfaces are initially generated by using an unsupervised tissue classifier to isolate a binary map of the cerebrospinal fluid in the MR image, and tiling the surface of the largest connected component inside the brain. There are a total of 3 zero points on each of the ventricular surfaces. Two of them are located at the middle part of the two "arms" (where the temporal and occipital horns join at the ventricular atrium), as shown by the large black dots in the second row. The third zero point is located in the middle of the model, where the frontal horns are closest to each other. Based on the computed conformal structure, we can partition the surface into 6 patches. Each patch can be conformally mapped to a rectangle. Although the two brain ventricle shapes are very different, the segmentation results are consistent in that the surfaces are partitioned into patches with the same relative arrangement and connectivity.

Not only are our results consistent on two different ventricle meshes, the bijective conformal mapping of each surface patch to rectangles in the parameter domain induces a parametric grid onto each surface, providing a way for direct surface matching between the two ventricles. One way to do this is to use a constrained harmonic map, $\phi : S_2 \to S_1$, where S_1 and S_2 are two surfaces to be matched. The basic pipeline is as follows: first we manually label the corresponding feature points. Then we Delaunay triangulate one segment based on the feature points, and induce the same triangulation for the corresponding segment of the second surface. By using a piecewise affine transformation, we map the second segment to the first one and denote the resulting mapping by ϕ_0. We improve the mapping by using a constrained harmonic map using the heat diffusion method, $\frac{\partial \phi(t)}{\partial t} = -\Delta\phi(t), \phi(0) = \phi_0$. After that, we resample the meshes using a regular grid in the parameter domain and construct new meshes with the same connectivity for the two segments.

It is difficult to find ϕ directly, but instead we can easily find a harmonic map between the parameter domains. Suppose the the conformal parameterization of S_1 is τ_1, conformal parameterization for S_2 is τ_2, then $\tau_1(S_1)$ and $\tau_2(S_2)$ are rectangles in R^2. We want to find a harmonic map $\tau : R^2 \to R^2$, such that $\tau \circ \tau_1(f_1^i) = \tau_2(f_2^i), \tau \circ \tau_1(\partial S_1) = \tau_2(\partial S_2), \Delta\tau = 0$, where Δ is the Laplacian operator defined on the plane. Then the map ϕ can be obtained by $\phi = \tau_1 \circ \tau \circ \tau_2^{-1}$. Because both τ_1 and τ_2 are conformal, τ is harmonic, and therefore ϕ is harmonic.

Once we get ϕ, we can explicitly compute the distance between two surfaces based on the surface correspondence by

$$E(S_1, S_2) = \frac{\int_{S_1} |\vec{r}_1 - \vec{r}_1 \circ \phi^{-1}| d\vec{r}}{\int_{S_1} d\vec{r}} \quad (2)$$

With Equation 2, we computed a surface distance between various examples of lateral ventricle and human face models. The upper row in Figure 4 shows three left brain lateral ventricular surfaces. The left two are for control subjects and the right one is for an HIV/AIDS patient. For each surface, we introduce three cuts and turn them into genus 2 surface and conformally map them to two rectangles. The distance between the left two surface is 10.05 and the distance between the right two is 13.85. It demonstrates the intra-class distance for control subjects is far less than the inter-class distance between control and HIV/AIDS classes. Thus our technique is useful to combine and compare 3D anatomical models across subjects or map functional imag-

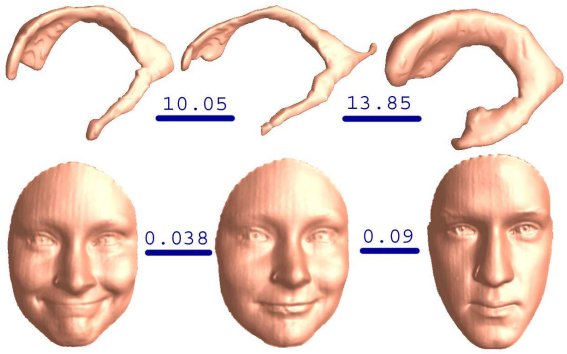

Figure 4. The brain lateral ventricular surface classification and face recognition results using our parameterization. The first row shows three left lateral ventricular surfaces in the brain. The left and middle surfaces are from control subjects and the right one is from an HIV/AIDS patient. On the second row, the left and middle faces are from the same person, with different expressions.

ing parameters onto anatomical surfaces.

The lower row in Figure 4 shows three face surfaces. The left two show the same person with different facial expressions. The second and third are two different individuals with a similar facial expression. For each face, we turn it into a genus 2 open boundary surface and conformally map them to two rectangles (as shown in Figure 2). The distance between the left two faces is 0.038 and the distance between the right two is 0.090. The distance between instances of the same person is much less than the distance between two different persons. This relative expression-invariance is an important requirement for metrics used in face recognition systems.

4. Conclusion and Future Work

In this paper, we presented a surface parameterization method that invokes the Riemann surface structure to generate conformal grids on surfaces of arbitrary complexity (including branching topologies). We applied it to human brain and face applications, as surface matching provides metrics for anatomical comparisons in brain mapping and face recognition. For high genus surfaces, a global conformal parameterization induces a canonical segmentation, i.e. there is a discrete partition of the surface into conformally parameterized patches. Each partition is either a topological disk or a cylinder and can be conformally mapped to a rectangle in the parameter domain. We demonstrated the parameterization for both closed and open boundary surfaces. The grid generation algorithm is intrinsic (i.e. does not depend on any initial choice of surface coordinates) and is stable, as shown by grids induced on ventricles of various shapes and sizes. Our work may introduce less distortion than other approaches and may be especially convenient for other post-processing work such as landmark matching. Our future work will focus on signal processing on general surfaces, as well as surface registration and shape and asymmetry analysis.

References

[1] R. Davies, C. Twining, T. Cootes, J. Waterton, and C. Taylor. A minimum description length approach to statistical shape modeling. *IEEE TMI*, 21(5):525–37, 2002.

[2] M. Desbrun, M. Meyer, and P. Alliez. Intrinsic parameterizations of surface meshes. In *Eurographics 2002*, volume 12, pages 209–218, 2002.

[3] M. S. Floater. Mean value coordinates. *CAGD*, 20(1):19–27, 2003.

[4] X. Gu, Y. Wang, T. Chan, P. Thompson, and S.-T. Yau. Genus zero surface conformal mapping and its application to brain surface mapping. *IEEE TMI*, 23(8):949–58, 2004.

[5] X. Gu and S.-T. Yau. Computing conformal structures of surfaces. *Communication of Information and Systems*, 2(2):121–46, 2002.

[6] X. Gu and S.-T. Yau. Global conformal surface parameterization. In *Proc. Eurographics/SIGGRAPH Symp. Geometry Processing*, pages 127–137. Eurographics Association, 2003.

[7] S. Haker, S. Angenent, A. Tannenbaum, R. Kikinis, G. Sapiro, and M. Halle. Conformal surface parameterization for texture mapping. *IEEE TVCG*, 6(2):181–189, 2000.

[8] M. K. Hurdal and K. Stephenson. Cortical cartography using the discrete conformal approach of circle packings. *NeuroImage*, 23:S119–S128, 2004.

[9] M. Jin, Y. Wang, S. Yau, and X. Gu. Optimal global conformal surface parameterization for visualization. In *IEEE Visualization*, pages 267–274, Austin, TX, Oct. 2004.

[10] B. Lévy, S. Petitjean, N. Ray, and J. Maillot. Least squares conformal maps for automatic texture atlas generation. In *SIGGRAPH 2002*, volume 21, pages 362–371, 2002.

[11] U. Pinkall and K. Polthier. Computing discrete minimal surfaces and their conjugate. In *Experimental Mathematics 2 (1)*, pages 15–36, 1993.

[12] E. Schwartz, A. Shaw, and E. Wolfson. A numerical solution to the generalized mapmaker's problem: Flattening nonconvex polyhedral surfaces. *IEEE TPAMI*, 11(9):1005–1008, 1989.

[13] A. Sheffer and E. Sturler. Parameterization of faceted surfaces for meshing using angle-based flattening. In *Engineering with Computers*, volume 17, pages 326–337, 2001.

[14] J.-P. Thirion. The extremal mesh and the understanding of 3D surfaces. *International Journal of Computer Vision*, 19(2):115–28, 1996.

[15] S. Zhang and P. Huang. High-resolution, real-time 3D shape acquisition. In *IEEE CVPR Workshop*, volume 3, page 28, Washington DC, USA, 2004.